

Anthropogenic contribution to global occurrence of heavy-precipitation and high-temperature extremes

Fischer, E. M.* , and R. Knutti

Institute for Atmospheric and Climate Science, ETH Zurich, Switzerland

*Corresponding author: Erich M. Fischer, Institute for Atmospheric and Climate Science, ETH Zurich, Universitätstrasse 16, 8092 Zurich, Switzerland. (erich.fischer@env.ethz.ch)

Two-step attribution and evaluation of changes in temperature and precipitation extremes

There is a serious lack of long-term, homogenous daily temperature and precipitation series with global coverage, which prevents us from performing a comprehensive observation-based assessment of hemispheric to global changes in the occurrence of extremes since the pre-industrial period. Thus, we here perform a two-step attribution approach based on the robust evidence that the observed global temperature increase can be largely attributed to human influence [Bindoff *et al.*, 2013 and references therein]. Like in previous single event attribution studies, the attribution of the change in the occurrence of extremes in response to a global mean temperature increase needs to be based on climate models. However, we here use the observational data available to evaluate changes in extremes in climate models and to demonstrate that simulated changes in extremes are consistent with the available observational record for the last six decades. Recent studies have demonstrated that despite certain limitations, CMIP5 models capture the general characteristics of temperature and precipitation extremes as well as their observed trends reasonably well [Fischer and Knutti, 2014; Min *et al.*, 2011; Sillmann *et al.*, 2014; Sillmann *et al.*, 2013; Zhang *et al.*, 2013; Zwiers *et al.*, 2011]. Some of the under- or overestimation of the observed trends in extremes may simply relate to biases in the simulated global mean temperature increase.

Thus, we here directly evaluate the change in temperature and precipitation extremes per degree global warming for the period and for the indices for which data is available. Figure S1 illustrates changes in

global average hot extremes (TXx, hottest day per year) and heavy precipitation extremes (Rx1day, wettest day per year) as a function of global mean temperatures in models and observations. We find that multi-model mean changes in hot and heavy precipitation extremes over the last six decades are similar to the observed trends in the two gridded observational data sets GHCNDEX and HADDEX2 [Donat *et al.*, 2013]. While individual models over- or underestimate the trend in hot and heavy precipitation extremes per degree warming, the multi-model mean is roughly within the range of internal variability of observed trends in heavy precipitation and temperature extremes. For the period considered the trend in hot extremes (TXx) per degree global warming is slightly overestimated by the models and the trend in heavy precipitation intensity (Rx1day) slightly underestimated as previously pointed out [Christidis *et al.*, 2011; Fischer and Knutti, 2014; Min *et al.*, 2011; Zwiers *et al.*, 2011]. In addition to a consistent trend in global averages of extremes, we further find that also the spatial probability distribution of simulated 50-yr trends in hot and heavy precipitation extremes in models are broadly consistent with observations [see Fischer and Knutti, 2014].

Finally, we find that the global transient FAR and PR estimate for hot extremes as well as their spatial patterns in the models are remarkably similar to those obtained by shifting the daily temperature climatology of the ERA interim analysis covering the period 1979-2010. Thus, we find no evidence for a bias in PR/FAR estimates due to a substantial over- or underestimation of climatological temperature variability, which is consistent with the evaluation of the previous generation of models in CMIP3 [Ylhaisi and Raisanen, 2014].

In summary the different lines of evidence presented here increase our confidence that the model-based link between changes in the occurrence of extremes and global temperature increase and thus the global average estimates for PR and FAR are consistent with the observational evidence available.

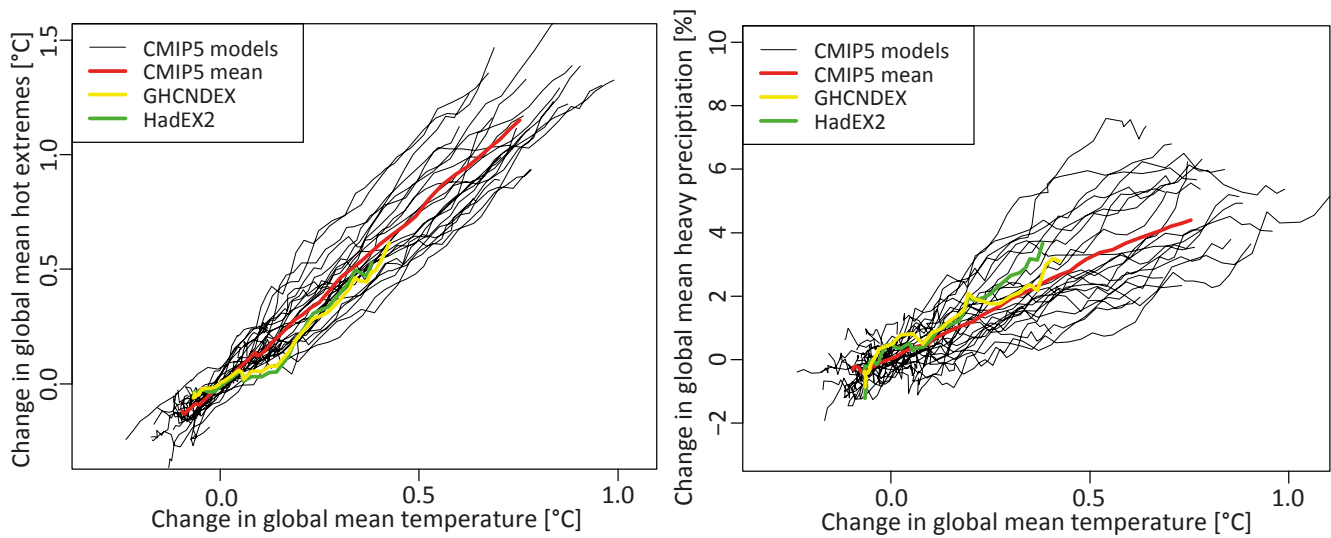


Fig. S1 | Evaluation of changes in temperature and precipitation extremes per degree global warming. 20-yr running means of global average (left) hot extremes, TX_x , and (right) heavy precipitation extremes, $Rx1day$, versus global mean temperature change for the period (1956-2010) as simulated by the individual CMIP5 models (black) and their multi-model mean (red), and as observed in the GHCNDEX data (yellow) and HadEX2 observational data (green). 20-yr running means for GHCNDEX and HadEX2 are plotted against observed global mean (land and ocean) from HadCRUT4. Observations and simulations are expressed as anomalies with respect to the reference period 1961-90. The model data for the extremes is masked to the area for which observational data is available and limited to latitudes between 66°S to 66°N .

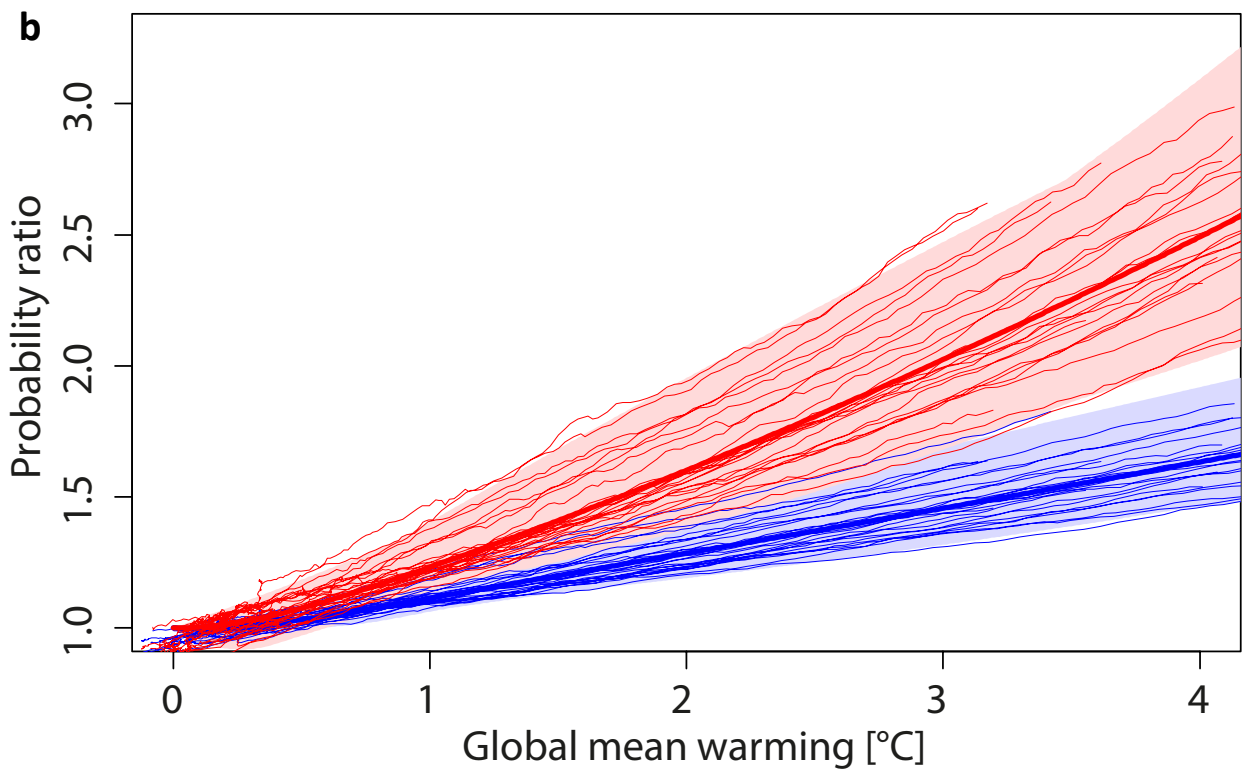
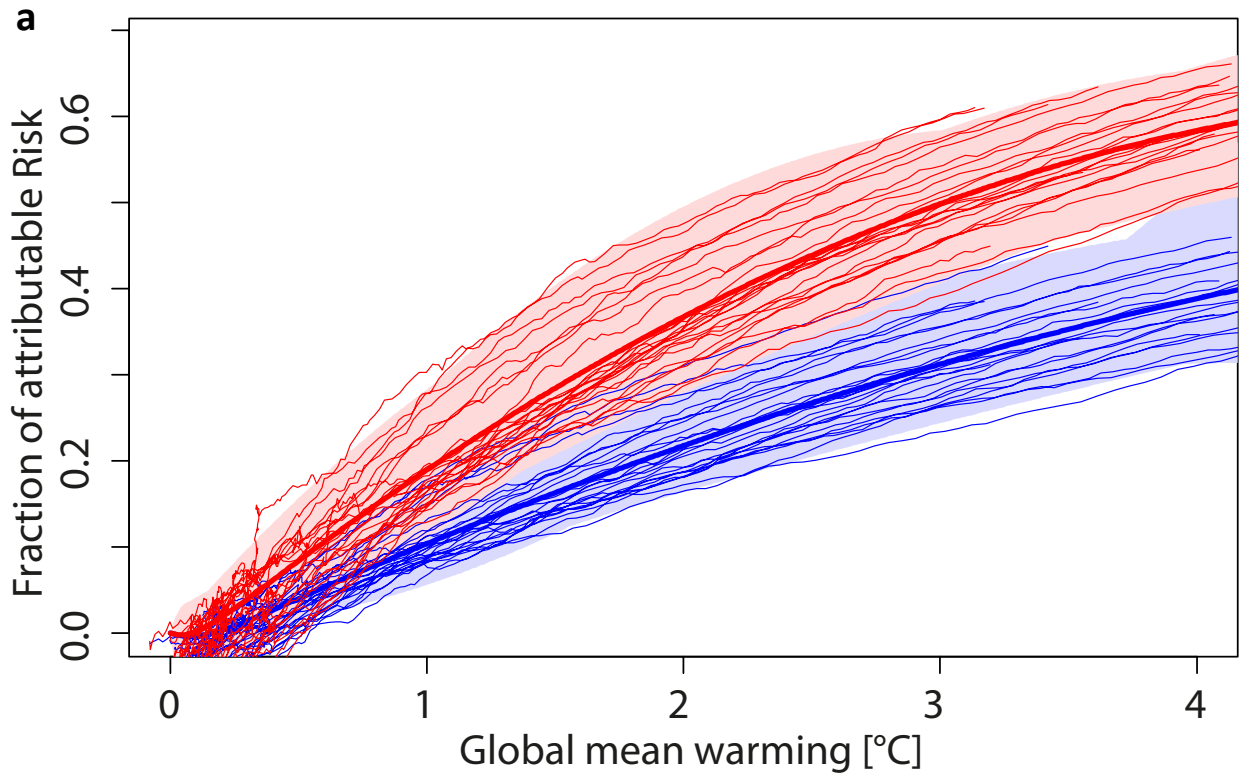
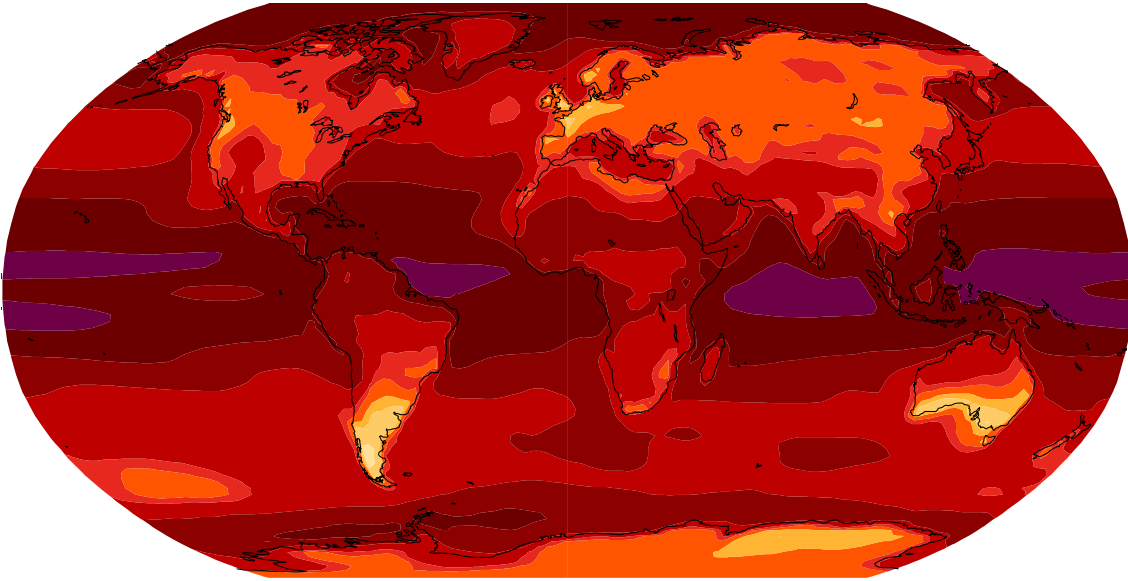


Fig. S2 | Heavy precipitation PR and FAR estimates for Northern mid to high latitudes. a-b, Same as Fig.2c and Fig. 2a but for mid-latitude land regions of the Northern Hemisphere (35°-66°N).

a PR estimated by shifting pre-industrial distribution by a local annual warming consistent with 2°C



b Simulated PR at 2°C warming

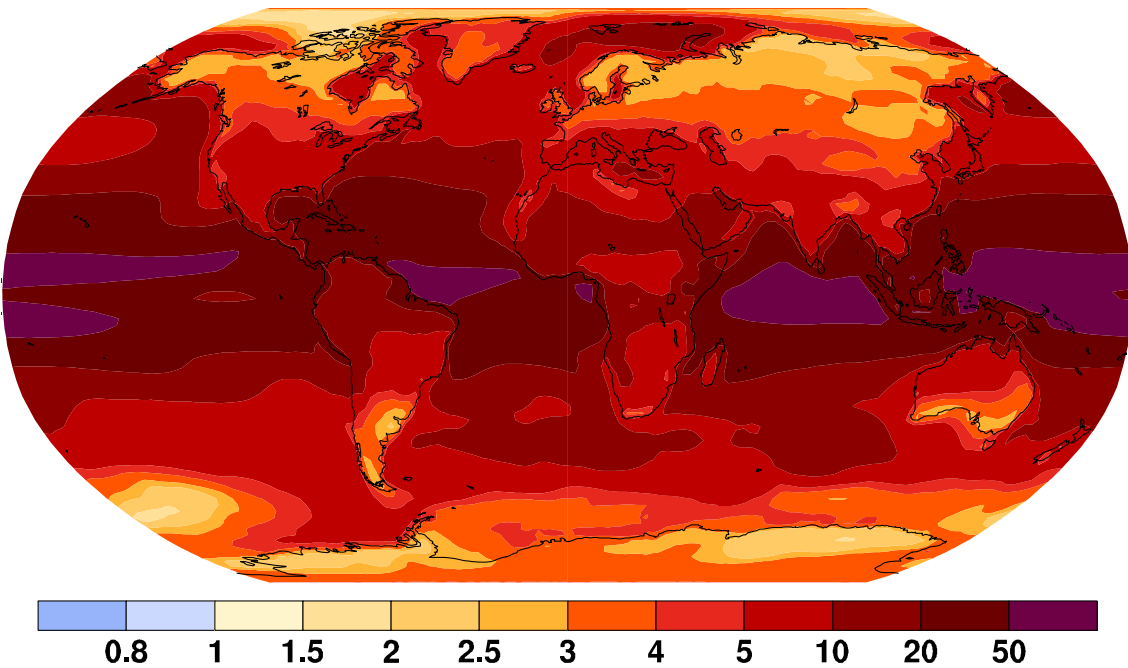


Fig. S3 | Estimated versus simulated probability ratio of hot extremes at 2°C warming. (a) Multi-model mean probability ratio of exceeding the pre-industrial 99th percentile estimated by shifting the pre-industrial temperature distribution as represented by the control simulation by the local annual mean temperature change. The latter is the difference between the local mean difference across the 30-yr period in which the model shows a global mean warming of 2°C and the pre-industrial period. (b) Same as Fig.3e, multi-model mean probability ratio determined from the transient simulations.

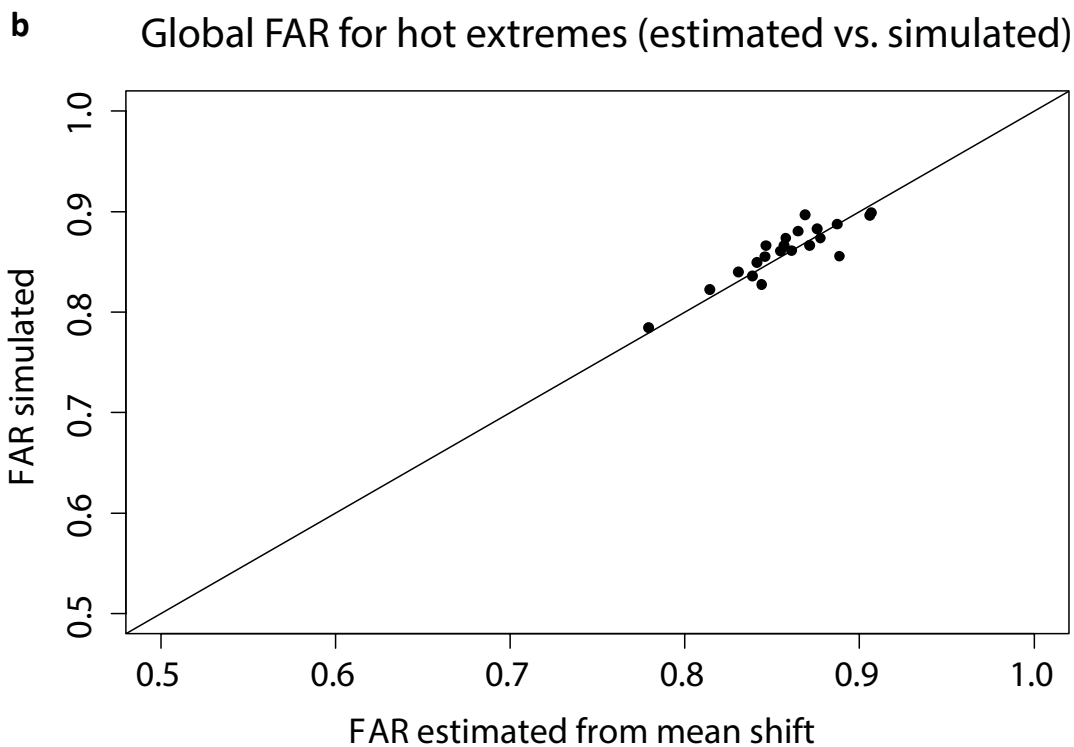
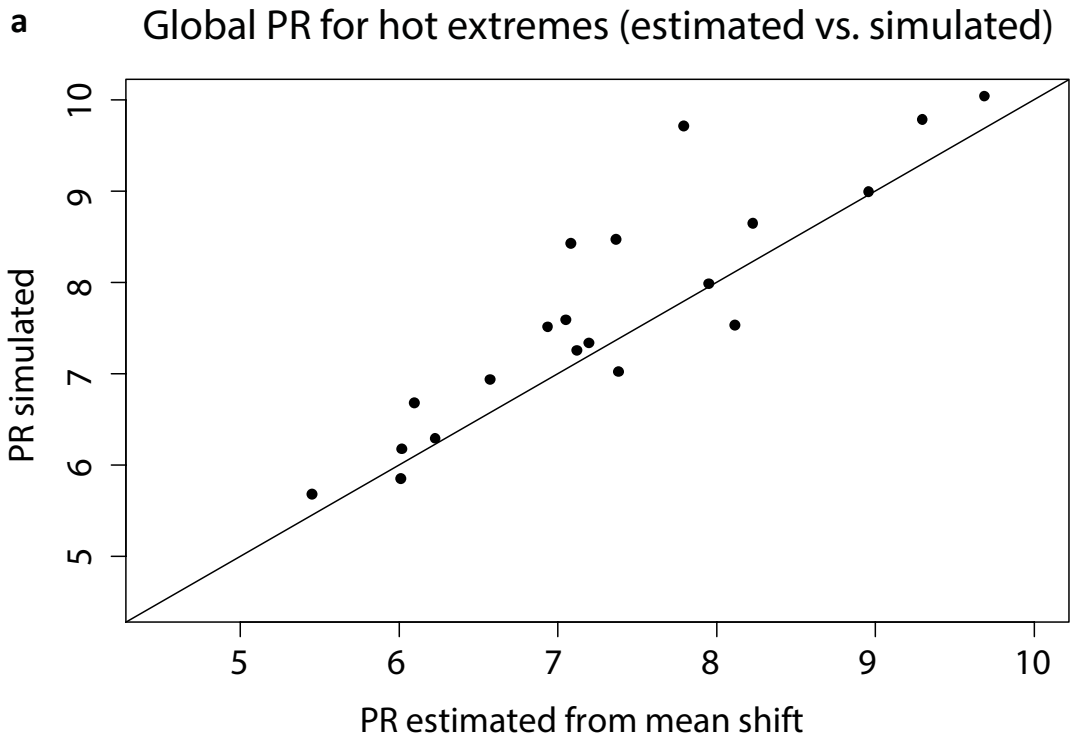


Fig. S4 | Estimated versus simulated global mean PR and FAR for hot extremes at 2°C warming. (a) Global land average of probability ratio at 2°C warming estimated from shifting the pre-industrial temperature distribution vs. simulated with the climate models (see Fig.S3). Each dot shows the estimated and simulated PR for one model. (b) Same but for FAR rather than PR.

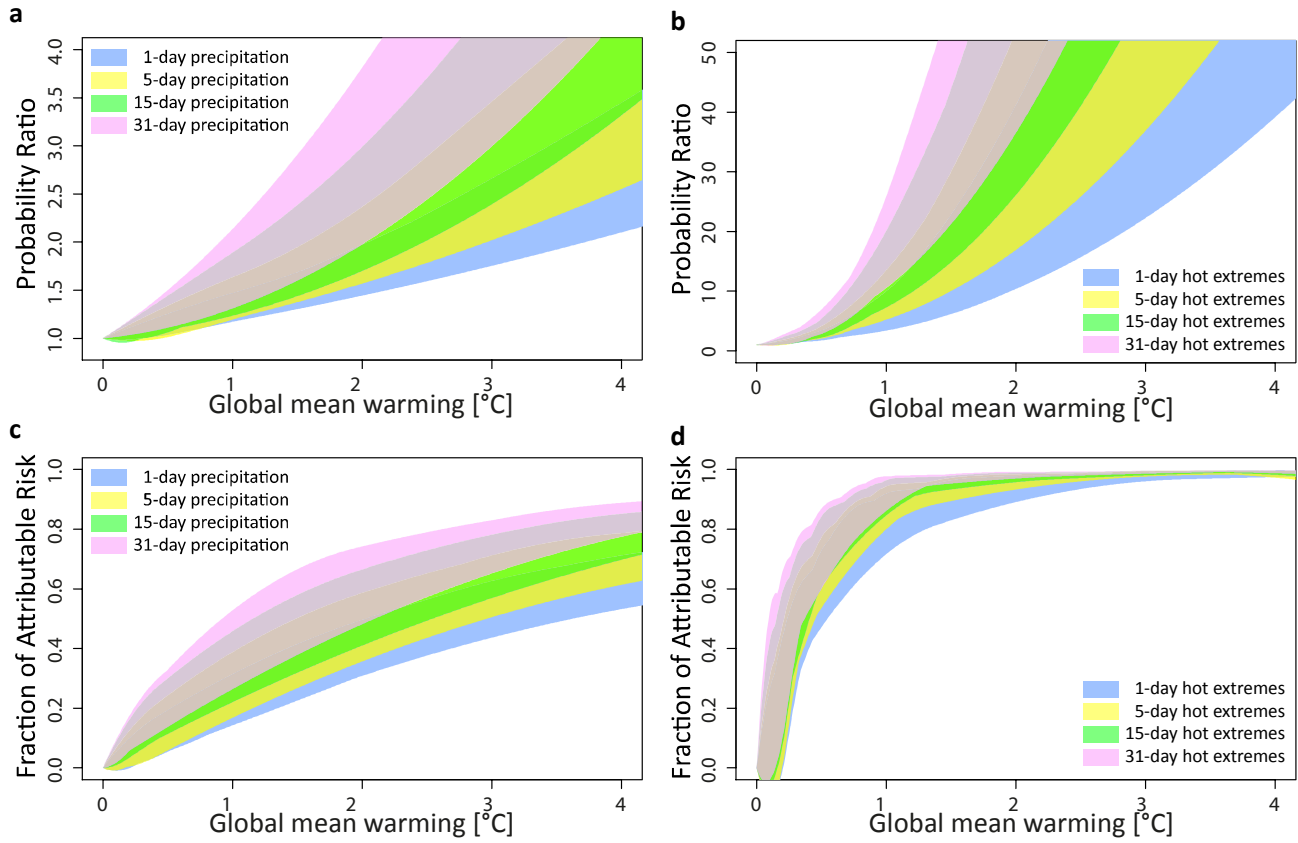


Fig. S5 | Probability ratio and FAR for multi-day temperature and precipitation extremes. (a-b) Probability ratio and (c-d) Fraction of Attributable Risk for 1-day, 5-day, 15-day, and 31-day (a, c) precipitation and (b, d) temperature extremes exceeding the pre-industrial 99.9% quantile at a given warming level. Multi-day events are calculated by applying a running mean to the daily data and repeating the analysis described above on the distribution of multi-day running means.

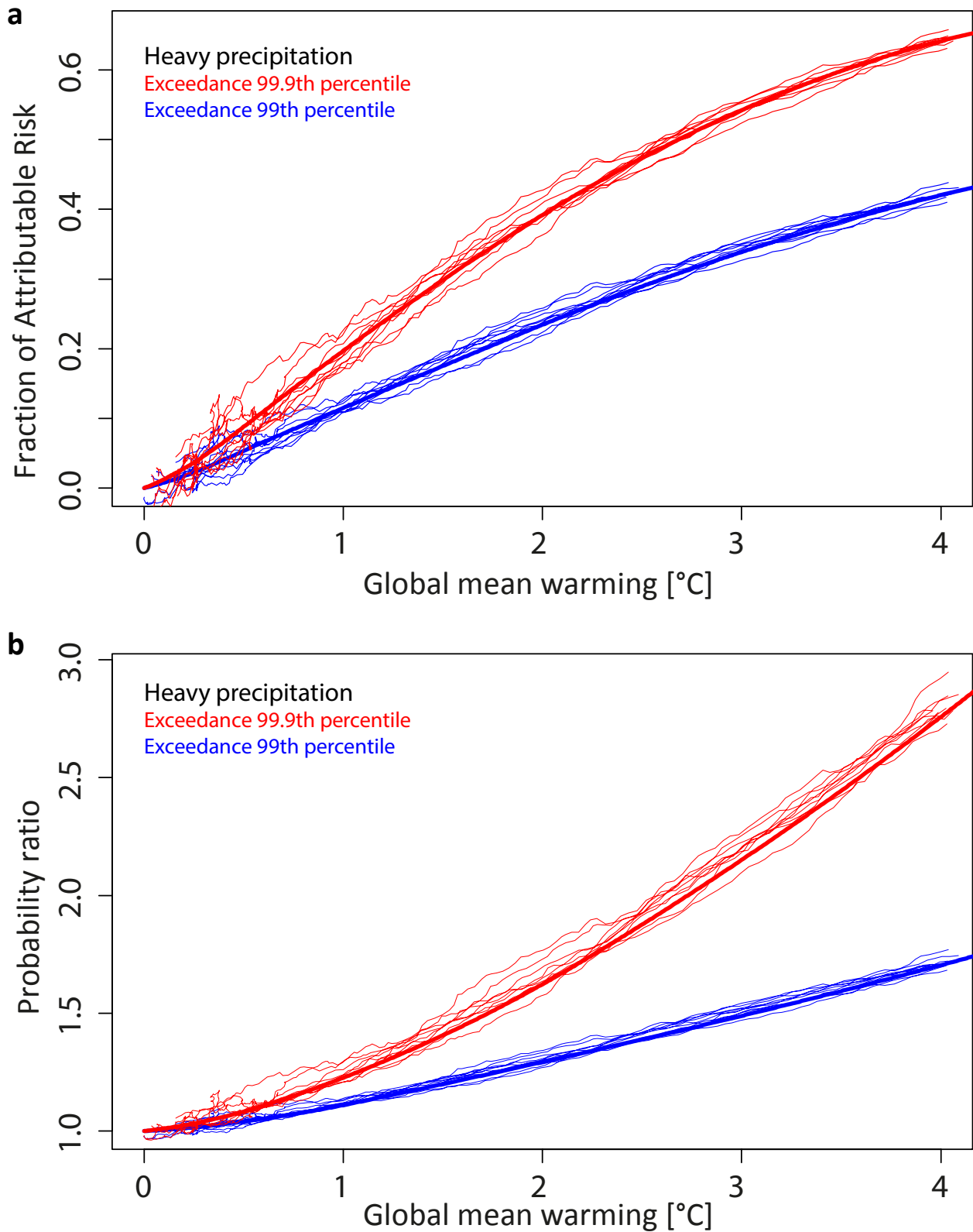


Fig. S6 | Uncertainty in heavy precipitation PR and FAR estimates induced by internal variability. Same as Fig.2a and Fig. 2c but based on 9 members of the NCAR-DOE CESM model. The different members of the model are initialized from different starting points in the pre-industrial control simulation and thereby have different ocean, sea-ice, land and atmospheric initial conditions.

Table S1 | Global climate models used in this study: *Table of 25 CMIP5 models analysed in this study. Daily output temperature at 2m and precipitation are used for the historical runs (all forcings), and RCP8.5 simulations.*

CMIP5 models used

ACCESS1-0	HadGEM2-CC
ACCESS1-3	HadGEM2-ES
bcc-csm1-1	inmcm4
bcc-csm1-1-m	IPSL-CM5A-LR
CanESM2	IPSL-CM5A-MR
CESM1-BGC	MIROC5
CMCC-CM	MIROC-ESM
CMCC-CMS	MIROC-ESM-CHEM
CNRM-CM5	MPI-ESM-LR
CSIRO-Mk3-6-0	MPI-ESM-MR
EC-EARTH	MRI-CGCM3
GFDL-ESM2G	NorESM1-M
GFDL-ESM2M	

Table S2 | Multi-model mean FAR estimates for heavy precipitation extremes in different seasons. *Multi model mean estimate for heavy precipitation (99.9th percentile) over the northern mid-latitudes (35-66°N) and high-latitudes (66-90°N) for annual mean, summer (JJA) and winter (DJF) for the 30-yr period showing a 2°C annual global mean warming. FAR estimates for precipitation are only robust for large regions and relatively strong warming signals.*

Precipitation extremes

Region	Annual	JJA	DJF
Northern mid-latitudes	0.38	0.35	0.54
Northern high-latitudes	0.46	0.50	0.60

Table S3 | Multi-model mean FAR estimates for hot extremes in different regions. *Multi model mean estimate for hot extremes (99.9th percentile) for the following regions: Europe, 30-75°N, 10°W-40°E; North America, 12-66°N, 60-170°W; South America 12°N-62°S, 34-82°W; Asia 5-75°N, 40-180°E; Africa 30°N-35°S, 20°W-52°E; Australia 11-45°S, 110-155°E. The FAR estimates are given for the 30-yr period showing a 0.85°C and 2°C annual global mean warming, respectively.*

Temperature extremes

Region	0.85°C	2.0°C
Europe	0.63	0.93
N America	0.67	0.94
S America	0.88	0.98
Asia	0.72	0.94
Africa	0.89	0.98
Australia	0.69	0.94

References

- Bindoff, N. L., et al. (2013), Detection and Attribution of Climate Change: from Global to Regional, in *Climate Change 2013: The Physical Science Basis. Contribution of Working Group I to the Fifth Assessment Report of the Intergovernmental Panel on Climate Change*, edited by T. F. Stocker, D. Qin, G. K. Plattner, M. Tignor, S. K. Allen, J. Boschung, A. Nauels, Y. Xia, V. Bex and P. M. Midgley, Cambridge University Press, Cambridge, United Kingdom and New York, NY, USA.
- Christidis, N., P. Stott, and S. Brown (2011), The Role of Human Activity in the Recent Warming of Extremely Warm Daytime Temperatures, *Journal of Climate*, 24(7), 1922-1930.
- Donat, M. G., et al. (2013), Updated analyses of temperature and precipitation extreme indices since the beginning of the twentieth century: The HadEX2 dataset, *Journal of Geophysical Research-Atmospheres*, 118(5), 2098-2118.
- Fischer, E. M., and R. Knutti (2014), Detection of spatially aggregated changes in temperature and precipitation extremes, *Geophysical Research Letters*, 41(2), 547-554.
- Min, S.-K., X. Zhang, F. W. Zwiers, and G. C. Hegerl (2011), Human contribution to more-intense precipitation extremes, *Nature*, 470(7334), 378-381.
- Sillmann, J., M. G. Donat, J. C. Fyfe, and F. W. Zwiers (2014), Observed and simulated temperature extremes during the recent warming hiatus, *Environmental Research Letters*, 9(6), 064023.
- Sillmann, J., V. Kharin, X. Zhang, F. Zwiers, and D. Bronaugh (2013), Climate extremes indices in the CMIP5 multimodel ensemble: Part 1. Model evaluation in the present climate, *Journal of Geophysical Research-Atmospheres*, 118(4), 1716-1733.
- Ylhaisi, J. S., and J. Raisanen (2014), Twenty-first century changes in daily temperature variability in CMIP3 climate models, *International Journal of Climatology*, 34(5), 1414-1428.
- Zhang, X., H. Wan, F. W. Zwiers, G. C. Hegerl, and S. K. Min (2013), Attributing intensification of precipitation extremes to human influence, *Geophysical Research Letters*, 10.1002/grl.51010.
- Zwiers, F., X. Zhang, and Y. Feng (2011), Anthropogenic Influence on Long Return Period Daily Temperature Extremes at Regional Scales, *Journal of Climate*, 24(3), 881-892.